Corresponding author:
Eyyüp Sabri Özden, M.D.
Department of Anesthesiology and
Reanimation, Faculty of Medicine, Suleyman
Demirel University Hospital, Çünür, East
Campus, 32260 Isparta, Turkey
Tel: +90-532-4529236
Fax: +90-246-2112083
Email: eyyupozden@sdu.edu.tr
ORCID: https://orcid.org/0000-0002-8070-0159

Dexpanthenol protects against lipopolysaccharide-induced acute kidney injury by restoring aquaporin-2 levels via regulation of the silent information regulator 1 signaling pathway

Eyyüp Sabri Özden[1], Halil Aşcı[2], Halil İbrahim Büyükbayram[3], Mehmet Abdulkadir Sevük[2], Orhan Berk İmeci[2], Hatice Kübra Doğan[4], Özlem Özmen[5]

Departments of [1]Anesthesiology and Reanimation, [2]Pharmacology, [3]Biochemistry, Faculty of Medicine, Suleyman Demirel University, Isparta, [4]Department of Bioengineering, Institute of Science, Suleyman Demirel University, Isparta, [5]Department of Pathology, Faculty of Veterinary Medicine, Mehmet Akif Ersoy University, Burdur, Turkey

Background: Acute kidney injury (AKI) is a serious pathology that causes dysfunction in concentrating urine due to kidney damage, resulting in blood pressure dysregulation and increased levels of toxic metabolites. Dexpanthenol (DEX), a pantothenic acid analog, exhibits anti-inflammatory and anti-apoptotic properties in various tissues. This study investigated the protective effects of DEX against systemic inflammation-induced AKI.

Methods: Thirty-two female rats were randomly assigned to the control, lipopolysaccharide (LPS), LPS+DEX, and DEX groups. LPS (5 mg/kg, single dose on the third day, 6 h before sacrifice) and DEX (500 mg/kg/day for 3 days) were administered intraperitoneally. After sacrifice, blood samples and kidney tissues were collected. Hematoxylin and eosin, caspase-3 (Cas-3), and tumor necrosis factor alpha (TNF-α) staining were performed on the kidney tissues. The total oxidant status (TOS) and total antioxidant status were measured using spectrophotometric methods. Aquaporin-2 (*AQP-2*), silent information regulator 1 (*SIRT1*), and interleukin-6 (*IL-6*) were detected using quantitative reverse transcription-polymerase chain reaction analysis.

Results: Histopathological analysis revealed that DEX treatment ameliorated histopathological changes. In the LPS group, an increase in the blood urea nitrogen, creatinine, urea, *IL-6*, Cas-3, TNF-α, and TOS levels and oxidative stress index was observed compared with the control group, whereas *AQP-2* and *SIRT1* levels decreased. DEX treatment reversed these effects.

Conclusions: DEX was found to effectively prevent inflammation, oxidative stress, and apoptosis in the kidneys via the *SIRT1* signaling pathway. These protective properties suggest DEX's potential as a therapeutic agent for the treatment of kidney pathologies.

Keywords: Apoptosis; Caspase 3; Dexpanthenol; Kidney; Oxidative stress; Sirtuin 1.

Introduction

Lipopolysaccharide (LPS) is an oligosaccharide extracted from the cell wall of Gram-negative bacteria that initiates the production and release of cytokines and subsequent

inflammatory processes [1]. LPS interacts with toll-like receptor-4 (TLR-4) located on the surface of the host cell, inducing the secretion of various proinflammatory cytokines such as tumor necrosis factor-alpha (TNF-α) [2]. This leads to the development of an inflammatory mechanism that could become systemic depending on the severity and/or duration. The kidneys, which are important elimination organs that receive the majority of blood, are also affected by this condition [3].

Acute kidney injury (AKI) is a clinical condition characterized by the sudden loss of kidney function, leading to an inability to eliminate urea and other nitrogenous waste products from the body along with alterations in extracellular fluid volume and electrolyte composition [4]. AKI can be caused by systemic inflammation, which is responsible for pathological changes, such as hyperemia, hemorrhage, and degeneration of tubular epithelial cells in the renal parenchyma [5]. This condition results in a decrease in glomerular filtration capacity and an increase in urea, blood urea nitrogen (BUN), and creatinine (Cr) levels due to impaired kidney function caused by inflammation [6].

Various water channels play a role in the development of clinical findings in renal pathology. Aquaporin-2 (*AQP-2*), a type of water channel found in the kidneys, plays a critical role in maintaining body water homeostasis [7]. The deficiency of *AQP-2* is observed in various kidney pathologies such as AKI, diabetic nephropathy, nephrogenic diabetes insipidus, polycystic kidney disease, and renal cell carcinoma [8]. The existing literature indicates that restoration of *AQP-2* levels through silent information regulator 1 (*SIRT1*) can alleviate kidney damage caused by inflammation [9].

SIRT1 is a member of the NAD+-dependent class III deacetylase family. The regulation of *SIRT1* expression is involved in various biological processes such as inflammation, oxidative stress, and apoptosis [10]. Thus, decreased *SIRT1* levels caused by inflammation may trigger oxidative stress and apoptosis. Tissue damage results in the formation of reactive oxygen species (ROS) that attempt to react and stabilize [11]. In pathological conditions where the antioxidant response, expressed as the total antioxidant status (TAS), is inadequate, the total oxidant status (TOS) increases, leading to oxidative stress [12]. A reduction in *SIRT1* activation results in oxidative stress. Consequently, apoptosis cannot be prevented, leading to controlled cell death. Apoptosis occurs when a cell loses its capacity to prevent the spread of cellular dysfunction and damage. The caspase family of proteins is involved in apoptosis and regulated by *SIRT1* [13]. This signaling pathway operates differently according to the intrinsic or extrinsic pathway of apoptosis, ultimately leading to cell death with caspase-3 (Cas-3) as the crucial mediator [14].

Dexpanthenol (DEX) is a biologically active alcohol analog of pantothenic acid that is converted into pantothenic acid in tissues. Studies have shown that DEX has anti-inflammatory, antioxidant, and anti-apoptotic effects in various tissues [15,16]. The potential relationship between DEX and *SIRT1*, which plays a role in the development of all pathologies associated with kidney damage, raises intriguing questions. This study aimed to demonstrate the relationship between DEX and *SIRT1* and determine the protective effects of DEX on the kidneys via the *SIRT1/AQP-2* signaling pathway.

Materials and Methods

Ethical approval

All experiments conducted in this study were performed in accordance with the National Institutes of Health guidelines for animal research and approved by the Suleyman Demirel University Isparta Committee on Animal Research (Approval No. 2022-06/72). This study was supported by the Scientific Research Fund of Suleyman Demirel University, under Project Number TSG-2020-8134.

Study animals and design

The sample size was calculated using the G Power 3.1.9.7 program (Heinrich-Heine-Universität Düsseldorf, Germany) with the following parameters: effect size = 0.4, alpha = 0.05, expected power (1-beta) = 0.80, and number of groups = 8.

Thirty-two adult female Wistar albino rats weighing 300–350 g were placed in a room under controlled temperature (21–22°C) and humidity (60% ± 5%) conditions, with a 12:12 h light/dark cycle. All the rats were fed a standard commercial chow diet (Korkuteli Yem, Turkey).

The rats in the control group (n = 8) received 1 ml of saline intraperitoneally (IP) once a day for three days in the left inguinal region and a single dose of 1 ml saline IP in the right inguinal region 30 min before the last dose of saline on the third day.

The rats in the LPS group (n = 8) received 1 ml of saline IP once a day for three days in the left inguinal region and a single dose of 5 mg/kg (0.5–1 ml) LPS (048K4126, Sigma Aldrich, USA) IP in the right inguinal region 30 min before the last dose of saline on the third day [17].

The rats in the LPS+DEX group (n = 8) received 1 ml of 500 mg/kg DEX (Bepanthen, Bayer, Turkey) IP once a day for three days in the left inguinal region and a single dose of 5 mg/kg (0.5–1 ml) LPS IP in the right inguinal region 30 min before the last dose

of DEX on the third day [18].

The rats in the DEX group (n = 8) received 1 ml of 500 mg/kg DEX IP once a day for three days in the left inguinal region and a single dose of 1 ml saline IP in the right inguinal region 30 min before the last dose of DEX on the third day.

Six hours after LPS (or saline for control and DEX groups) administration, all rats received 80–100 mg/kg ketamine (Ketalar, Pfizer, Turkey) and 8–10 mg/kg xylazine (XylazinBio 2%, Bioveta PLC, Czech Republic) to induce anesthesia. After anesthesia, the rats were sacrificed and blood samples were taken from the inferior vena cava through an abdominal incision. Half of the kidney specimens were stored at –20°C for biochemical analysis and –80°C for quantitative reverse transcription-polymerase chain reaction (qRT-PCR) analysis, while the remaining tissues were fixed with 10% buffered formalin for histopathological and immunohistochemical analysis. Experimental design has been visualized in Fig. 1.

Histopathological examination

Kidney specimens were fixed in a 10% buffered formalin solution. Samples were collected for routine pathological processing using an automatic tissue processor (Leica ASP300S, Leica Microsystems, Germany) and embedded in paraffin wax. Using a rotary microtome (Leica RM2155, Leica Microsystems), 5-μm thick sections were obtained from the paraffin blocks. The sections were then stained with hematoxylin and eosin (H&E), mounted on a coverslip, and examined under a light microscope.

Immunohistochemical examination

For immunohistochemical examination, two series of sections taken from all blocks of the kidneys were drawn on poly-L-lysine coated slides and stained immunohistochemically for Cas-3 (anti-caspase-3 antibody (E-8): sc-7272) and TNF-α (anti-TNFα antibody (52B83): sc-52746, 1/100 dilution) (Santa Cruz Biotechnology, Inc., USA) expression using the streptavidin biotin technique according to the manufacturer's instructions. The sections were incubated with primary antibodies for 60 min and immunohistochemistry was performed using biotinylated secondary antibodies and streptavidin-alkaline phosphatase conjugate. EXPOSE mouse- and rabbit-specific HRP/DAB detection IHC kits (ab80436) (Abcam, UK) were used as secondary antibodies. Diaminobenzidine (DAB) was used as the chromogen. For the negative controls, an antigen dilution solution was used instead of the primary antibody. All examinations were performed on blinded samples by a specialized pathologist from another university.

For immunohistochemical analysis, the sections were investigated separately for each antibody. To evaluate the severity of the immunohistochemical reaction of cells with markers, semi-quantitative analyses were performed using a grading score ranging from (0) to (3) as follows: (0) negative staining, (1) focal weak staining, (2) diffuse weak staining, and (3) diffuse strong staining. For evaluation, 10 different areas of each sections examined under 40x objective magnification. Morphometric analyses and microphotography were performed using the Database Manual cellSens Life Science Imaging Software (Olympus Opitical Co., Japan). The results were saved and statistically analyzed.

Measurement of blood parameters

The blood samples of all the individual rats (n = 32) were transferred into gel-containing tubes, and the sera were separated by centrifugation at 3,000 rpm for 10 min and aliquoted into three portions per serum. Samples were stored at –80°C until they were analyzed. Urea and Cr levels were measured spectrophotometri-
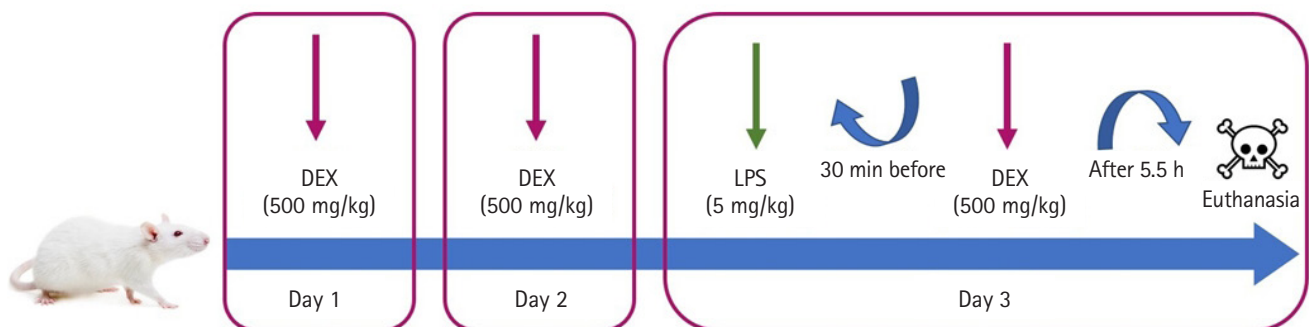

Fig. 1. Experimental design of the study. The experimental design, including the application times of LPS and DEX as well as the sacrifice time points. The study consisted of the control, LPS, LPS+DEX, and DEX groups, each containing eight animals. LPS: lipopolysaccharide, DEX: dexpanthenol.

cally with a Beckman Coulter AU 5800 autoanalyzer (Beckman Coulter, USA) using a kit compatible with the instrument (Beckman Coulter Urea/Urea Nitrogen assay kit, Beckman Coulter Creatinine assay kit) and BUN levels were calculated with the formula BUN = Urea/2.14.

Measurement of oxidative stress parameters

Kidney tissue samples were homogenized using the Ultra Turrax Janke & Kunkel T-25 homogenizer (IKA®-Werke GmbH & Co. KG, Germany) for oxidant-antioxidant analysis. The TAS and TOS were measured spectrophotometrically (AU 5800 autoanalyzer, Beckman Coulter) using commercial kits (Rel Assay Diagnostics, Turkey), and the oxidative stress index (OSI) was calculated using the following formula: OSI = TOS/TAS/10 [19]. For TAS analysis, antioxidants in the sample reduce dark blue-green colored 2,2'-azino-bis (3-ethylbenzothiazoline-6-sulfonic acid) (ABTS) radicals to their colorless ABTS form. The change in the absorbance at 660 nm was associated with the TAS level of the sample. This method determines the antioxidative effect of a sample against potent free radical reactions initiated by the production of hydroxyl radicals. The results are expressed as μmol Trolox Eqv/L [20].

For TOS analysis, oxidants present in the sample oxidize the ferrous ion-o-dianisidine complex to the ferric ion. Oxidation reactions are enhanced by glycerol molecules, which are abundant in the reaction medium. The ferric ions form a colored complex with xylenol orange in an acidic medium. The color intensity, which can be measured spectrophotometrically, has been found to be related to the total amount of oxidant molecules already present in the sample. The assay was calibrated with hydrogen peroxide, and the results were expressed in terms of micromolar hydrogen peroxide equivalents per liter (μmol H_2O_2 Eqv/L) [21].

Quantitative reverse transcription-polymerase chain reaction (RT-qPCR)

Total RNA was extracted from the tissues using TRIzol™ Reagent (#15596026, Thermo Fisher Scientific, Life Sciences Solutions, USA) according to the manufacturer's instructions. The quality of the RNA was determined using a nanospectrophotometer (#732-2533 VWR® mySPEC, Micro-Volume Spectrophotometers, VWR International GmbH, Austria). RNA (1 μg) was transcribed using the iScript cDNA Synthesis Kit with oligo-dT primers (Bio-Rad Laboratories, USA). The reaction mixture was incubated for 20 min at 46°C, 5 min at 25°C, and 1 min at 95°C. Real-time PCR amplification was performed using the SYBR Green Master Mix (Bio-Rad Laboratories) according to the manufacturer's instructions using a CFX96 instrument (Bio-Rad Laboratories). Specific primers were designed for the amplification of SIRT1, AQP-2, IL-6 (primer sequences provided upon request) and glyceraldehyde-3-phosphate dehydrogenase (GAPDH), and the cDNA samples for each PCR were analyzed in triplicate. GAPDH expression was used for normalization. Gene expression was relatively quantified using the comparative ΔΔCt method.

Statistical analysis

Statistical analyses between groups were performed using the SPSS 18.00 package program (SPSS Inc., USA) and the one-way analysis of variance (ANOVA) post hoc LSD test was used for the qRT-PCR, biochemical, histopathological, and immunohistochemical analyses. The Kruskal–Wallis test was used to identify any notable differences in the immunohistochemical analyses among the groups. Statistical significance was set at P < 0.05.

Results

Histopathological results

Histopathological examination revealed marked hyperemia, slight to moderate hemorrhage, and degeneration of tubular epithelial cells in kidney sections of the LPS group. In addition to inflammatory cell infiltration, DEX treatment decreased the pathological findings in the LPS+DEX group. Normal tissue histology was observed in the control and DEX groups (Fig. 2).

Immunohistochemical findings

Immunohistochemical examination showed increased Cas-3 and TNF-α expression in tubular cells in the LPS group. DEX treatment ameliorated these changes in the LPS+DEX group. Very low or negative expression was observed in the control and DEX groups (Figs. 3 and 4). The results of the statistical analyses are presented in Table 1.

Biochemical results

Urea, Cr, and BUN levels were measured biochemically to evaluate kidney function. All markers were significantly increased in the LPS group compared to the control group (P < 0.001, P < 0.01, and P < 0.001, respectively). DEX treatment significantly reversed these changes (P < 0.001, P < 0.01, and P < 0.001, respectively). All kidney function markers were found to be signifi-
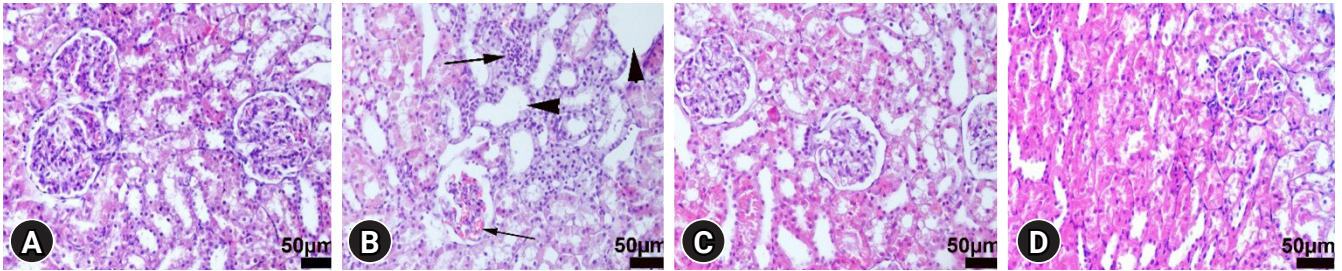
Fig. 2. Microscopical appearance of the kidneys among the groups. (A) Normal tissue histoarchitecture in the control group, rat number: 2. (B) Marked hyperemia in the glomerulus (thin arrow), inflammatory cell infiltrations (thick arrow), and cystic dilatations in the tubules (arrow heads) in the LPS group, rat number: 1. (C) Decreased pathological findings in the LPS+DEX group, rat number: 4. (D) Normal kidney histology in the DEX group, rat number: 6. HE, scale bars = 50 μm. LPS: lipopolysaccharide, DEX: dexpanthenol.
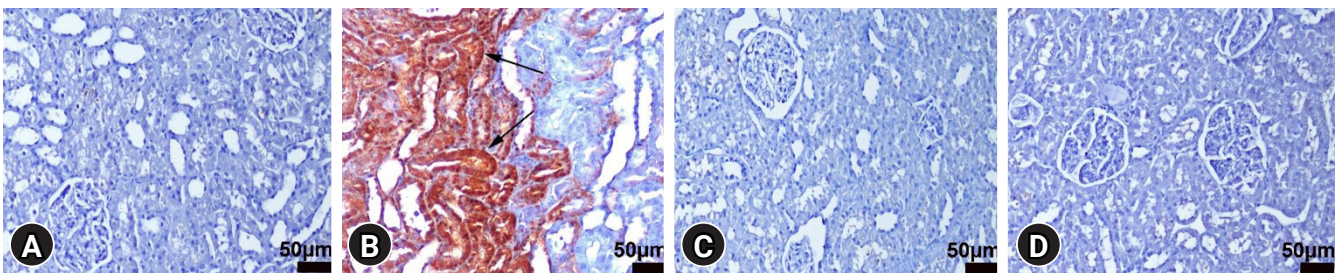

Fig. 3. Cas-3 immunohistochemical findings of the kidneys among the groups. (A) Negative expression in the control group, rat number: 3. (B) Marked increase in the expression (arrows) of tubular epithelial cells in the LPS group, rat number: 7. (C) Decreased expression in the LPS+DEX group, rat number: 3. (D) Negative expression in the DEX group, rat number: 2. Streptavidin biotin peroxidase method, scale bars = 50 μm. LPS: lipopolysaccharide, DEX: dexpanthenol.
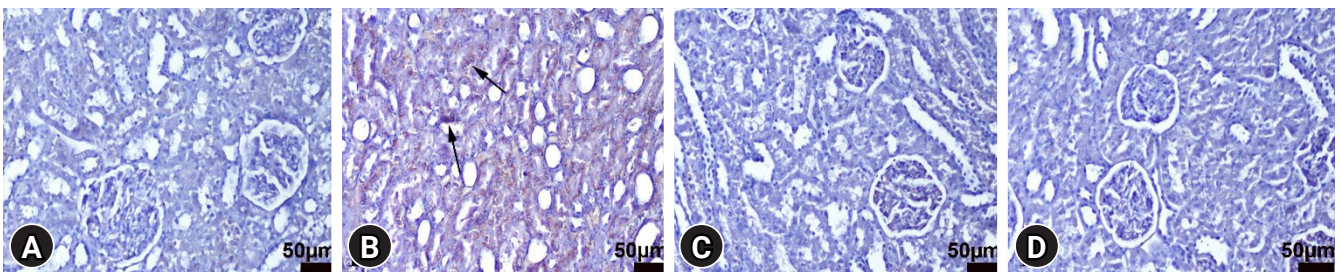

Fig. 4. TNF-α immunohistochemistry findings of the kidneys among the groups. (A) Negative expression in the control group, rat number: 1. (B) Increased expression (arrows) of the tubular epithelial cells in the LPS group, rat number: 2. (C) Decreased expression in the LPS+DEX group, rat number: 7. (D) Negative expression in the DEX group, rat number: 7. Streptavidin biotin peroxidase method, scale bars = 50 μm. LPS: lipopolysaccharide, DEX: dexpanthenol.

cantly lower in the DEX group than in the LPS group ($P < 0.001$, $P < 0.01$, and $P < 0.001$, respectively) (Fig. 5).

To indicate oxidative stress in the kidney tissues, TOS and TAS levels were measured, and the OSI was calculated. The increase in the LPS group was significant compared to the control group for TOS levels and the OSI ($P < 0.001$ for both). DEX treatment significantly reversed these effects ($P < 0.01$ and $P < 0.001$, respectively) (Fig. 6).

SIRT1, *AQP-2*, and *IL-6* levels were evaluated using qRT-PCR.

In the LPS group, *SIRT1* and *AQP-2* levels significantly decreased, whereas *IL-6* levels significantly increased ($P < 0.001$, $P < 0.01$, and $P < 0.01$, respectively). Although DEX treatment reversed these effects, only the increase in *AQP-2* was significant ($P < 0.01$). *IL-6* levels in the LPS+DEX group were significantly higher compared to the control group ($P < 0.05$). In the DEX group, *SIRT1* and *AQP-2* levels were the highest, while *IL-6* levels were the lowest (Fig. 7).

Table 1. Statistical Analysis Results of Immunohistochemical Scores between the Groups

Groups	Cas-3 scores	TNF-α scores
Control	0.37 ± 0.18	0.37 ± 0.18
LPS	2.75 ± 0.46*	2.00 ± 0.92*
LPS+DEX	0.87 ± 0.64†	1.37 ± 0.51*,†
DEX	0.25 ± 0.16†,‡	0.37 ± 0.18†,‡
P value	< 0.001	< 0.001

Values are presented as mean ± SD. LPS: lipopolysaccharide, DEX: dexpanthenol, Cas-3: caspase-3, TNF-α: tumor necrosis factor-alpha. *Represents comparison with control group, †represents comparison with LPS group, ‡represents comparison with LPS+DEX group.

Discussion

The interplay between systemic inflammation and endothelial and tubular cell injury is crucial for AKI pathogenesis [22]. The development of tubular dysfunction due to microvascular injury leads to disruption of renal excretion, thereby affecting the blood profile [23]. This can also result in the dysfunction of AQP channels as a consequence of tubular damage.

Systemic inflammation is a major cause of AKI and can trigger this pathological process [24]. This study aimed to demonstrate the therapeutic effects of DEX against renal damage induced by systemic inflammation.

The recognition of LPS by TLR-4 in systemic circulation triggers an immune response and leads to the release of inflammatory
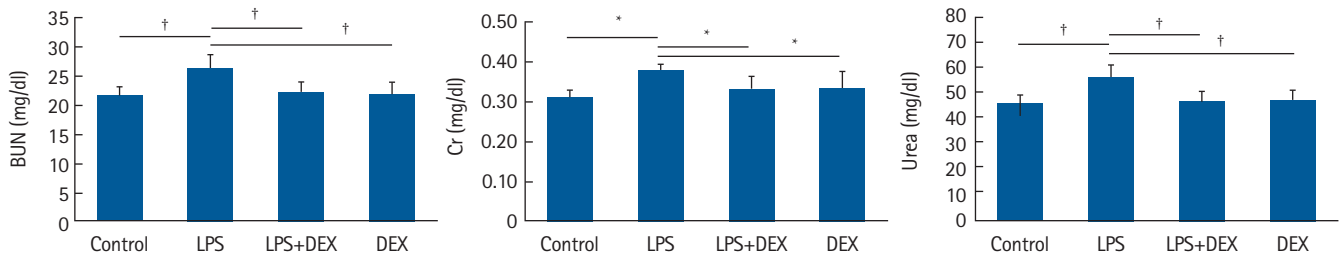

Fig. 5. BUN, Cr, and Urea levels. Values are presented as mean ± SD. LPS: lipopolysaccharide, DEX: dexpanthenol, BUN: blood urea nitrogen, Cr: creatinine. *P < 0.01, †P < 0.001.
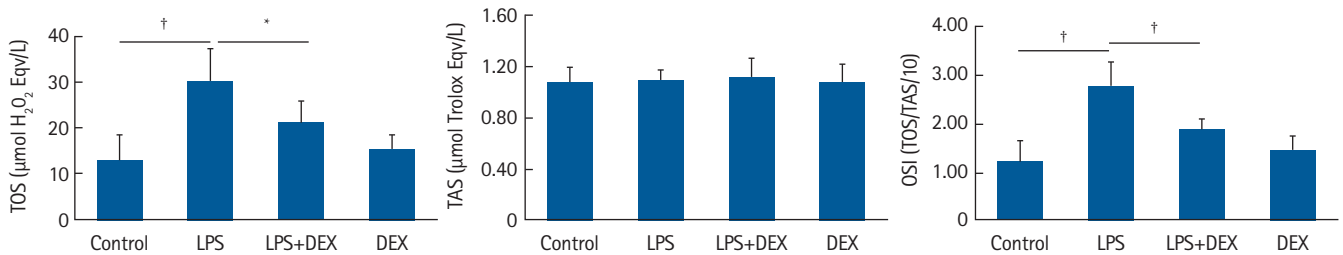

Fig. 6. Oxidative stress markers in kidney tissue. Values are presented as mean ± SD. LPS: lipopolysaccharide, DEX: dexpanthenol, TOS: total oxidant status, TAS: total antioxidant status, OSI: oxidative stress index. *P < 0.01, †P < 0.001.
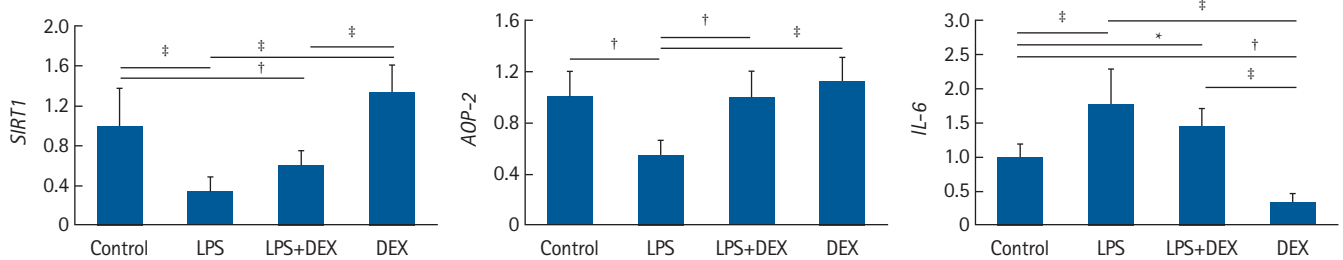

Fig. 7. Relative mRNA expressions of *SIRT1*, *AQP-2*, and *IL-6*. Values are presented as mean ± SD. LPS: lipopolysaccharide, DEX: dexpanthenol, *SIRT1*: silent information regulator 1, *AQP-2*: aquaporin-2, *IL-6*: interleukin-6. *P < 0.05, †P < 0.01, ‡P < 0.001.

cytokines [25]. Because the kidneys receive the most blood per unit of tissue, they are inevitably affected by this systemic event [26]. In our study, we observed that the levels of the most important inflammatory cytokines, TNF-α and *IL-6*, were elevated in the LPS group, and the potential treatment agent, DEX, reversed these effects owing to its anti-inflammatory activity. These findings are consistent with those of Bilgic et al. [27], who reported a significant decrease in TNF-α and *IL-6* levels following DEX treatment in a rat model of drug toxicity.

Although the molecular relationship between systemic inflammation and AKI is not fully understood, several mechanisms have been proposed. Tubular degeneration may significantly affect active and passive transport by impairing tubular integrity and water channel function, resulting in problems with the excretion of urea and similar metabolites from the kidneys. In this study, an increase in urea, BUN, and Cr levels was observed in the AKI model induced by inflammation, and an improvement was observed with DEX treatment.

Furthermore, previous studies have shown that decreased *AQP-2* levels are associated with kidney disease and that restoring *AQP-2* levels can have therapeutic effects [28]. Consistent with these findings, an increase in *AQP-2* levels in the DEX group compared with the LPS group was found in the current study. An in vitro study demonstrated that this increase was mediated by *SIRT1* and our results are consistent with these findings [29].

The association between inflammation and oxidative stress is well established, and microvascular damage may contribute to this process [30]. Microvascular damage can lead to the impairment of tubular function and tissue oxygenation, resulting in the generation of ROS that exacerbates inflammation and tissue damage [31]. The decrease in the OSI following DEX treatment in our study is thus consistent with previous study, which have reported that DEX decreases OSI in a model of amikacin-induced nephrotoxicity [18]. The imbalance in oxidative stress is dependent on an insufficient response of the *SIRT1* signaling pathway, which plays a crucial role in regulating inflammation and apoptosis. The decrease in *SIRT1* levels observed in the LPS group was associated with changes in inflammation, oxidative stress, and apoptosis markers, as evidenced by an increase in Cas-3 levels. Our findings suggest that DEX treatment restores *SIRT1* levels and exerts a curative effect against AKI-induced inflammation, oxidative stress, and apoptosis.

In conclusion, the results of this study suggest that DEX treatment can prevent the formation of damage mechanisms in AKI induced by systemic inflammation triggered by LPS by restoring *AQP-2* levels via the *SIRT1* signaling pathway, thus protecting the kidney structure in rats. Therefore, DEX may be a promising candidate for treating AKI and other kidney diseases associated with reduced *AQP-2* levels. However, the lack of significant changes in the group treated with DEX alone suggests the need for further studies assessing different durations and doses of DEX. Detailed molecular analyses are required to fully understand the mechanisms underlying the therapeutic effects of DEX on renal damage.

Funding

Conflicts of Interest

No potential conflict of interest relevant to this article was reported.

Data Availability

The datasets generated during and/or analyzed during the current study are available from the corresponding author on reasonable request.

Author Contributions

Eyyüp Sabri Özden (Conceptualization; Data curation; Investigation; Methodology; Project administration; Supervision; Validation; Visualization; Writing – original draft; Writing – review & editing)
Halil Aşcı (Conceptualization; Data curation; Funding acquisition; Investigation; Methodology; Project administration; Supervision; Validation; Visualization; Writing – original draft; Writing – review & editing)
Halil İbrahim Büyükbayram (Data curation; Formal analysis; Methodology; Resources; Software; Supervision; Validation; Visualization; Writing – original draft; Writing – review & editing)
Mehmet Abdulkadir Sevük (Data curation; Investigation; Project administration; Validation; Visualization; Writing – original draft; Writing – review & editing)
Orhan Berk İmeci (Data curation; Investigation; Project administration; Validation; Visualization; Writing – original draft; Writing – review & editing)
Hatice Kübra Doğan (Formal analysis; Methodology; Software; Writing – original draft; Writing – review & editing)
Özlem Özmen (Conceptualization; Data curation; Formal analysis; Methodology; Supervision; Validation; Visualization; Writing – original draft; Writing – review & editing)

ORCID

Eyyüp Sabri Özden, https://orcid.org/0000-0002-8070-0159

Halil Aşcı, https://orcid.org/0000-0002-1545-035X

Halil İbrahim Büyükbayram, https://orcid.org/0000-0003-0560-042X

Mehmet Abdulkadir Sevük, https://orcid.org/0000-0003-3875-9365

Orhan Berk İmeci, https://orcid.org/0000-0002-3850-0137

Hatice Kübra Doğan, https://orcid.org/0000-0002-6061-1300

Özlem Özmen, https://orcid.org/0000-0002-1835-1082

References

1. Ciesielska A, Matyjek M, Kwiatkowska K. TLR4 and CD14 trafficking and its influence on LPS-induced pro-inflammatory signaling. Cell Mol Life Sci 2021; 78: 1233-61.

2. Hoogland IC, Houbolt C, van Westerloo DJ, van Gool WA, van de Beek D. Systemic inflammation and microglial activation: systematic review of animal experiments. J Neuroinflammation 2015; 12: 114.

3. Scholz H, Boivin FJ, Schmidt-Ott KM, Bachmann S, Eckardt KU, Scholl UI, et al. Kidney physiology and susceptibility to acute kidney injury: implications for renoprotection. Nat Rev Nephrol 2021; 17: 335-49.

4. Levey AS, James MT. Acute kidney injury. Ann Intern Med 2017; 167: ITC66-ITC80. Erratum in: Ann Intern Med 2018; 168: 84.

5. Legrand M, Bell S, Forni L, Joannidis M, Koyner JL, Liu K, et al. Pathophysiology of COVID-19-associated acute kidney injury. Nat Rev Nephrol 2021; 17: 751-64.

6. Ronco C, Bellomo R, Kellum JA. Acute kidney injury. Lancet 2019; 394: 1949-64.

7. Su W, Cao R, Zhang XY, Guan Y. Aquaporins in the kidney: physiology and pathophysiology. Am J Physiol Renal Physiol 2020; 318: F193-203.

8. He J, Yang B. Aquaporins in renal diseases. Int J Mol Sci 2019; 20: 366.

9. Alam F, Syed H, Amjad S, Baig M, Khan TA, Rehman R. Interplay between oxidative stress, SIRT1, reproductive and metabolic functions. Curr Res Physiol 2021; 4: 119-24.

10. Singh V, Ubaid S. Role of silent information regulator 1 (SIRT1) in regulating oxidative stress and inflammation. Inflammation 2020; 43: 1589-98. Erratum in: Inflammation 2021; 44: 2142.

11. Minutoli L, Puzzolo D, Rinaldi M, Irrera N, Marini H, Arcoraci V, et al. ROS-mediated NLRP3 inflammasome activation in brain, heart, kidney, and testis ischemia/reperfusion injury. Oxid Med Cell Longev 2016; 2016: 2183026.

12. Xie D, Hu J, Yang Z, Wu T, Xu W, Meng Q, et al. Vitamin supplementation protects against nanomaterial-induced oxidative stress and inflammation damages: a meta-analysis of in vitro and in vivo studies. Nutrients 2022; 14: 2214.

13. Wang XL, Wu LY, Zhao L, Sun LN, Liu HY, Liu G, et al. SIRT1 activator ameliorates the renal tubular injury induced by hyperglycemia in vivo and in vitro via inhibiting apoptosis. Biomed Pharmacother 2016; 83: 41-50.

14. Ouyang Z, Yang B, Yi J, Zhu S, Lu S, Liu Y, et al. Exposure to Fluoride induces apoptosis in liver of ducks by regulating Cyt-C/Caspase 3/9 signaling pathway. Ecotoxicol Environ Saf 2021; 224: 112662.

15. Li-Mei W, Jie T, Shan-He W, Dong-Mei M, Peng-Jiu Y. Anti-inflammatory and anti-oxidative effects of dexpanthenol on lipopolysaccharide induced acute lung injury in mice. Inflammation 2016; 39: 1757-63.

16. Shin JY, Kim J, Choi YH, Kang NG, Lee S. Dexpanthenol promotes cell growth by preventing cell senescence and apoptosis in cultured human hair follicle cells. Curr Issues Mol Biol 2021; 43: 1361-73.

17. Cao C, Gao T, Cheng M, Xi F, Zhao C, Yu W. Mild hypothermia ameliorates muscle wasting in septic rats associated with hypothalamic AMPK-induced autophagy and neuropeptides. Biochem Biophys Res Commun 2017; 490: 882-8.

18. Doğan EE, Erkoç R, Ekinci İ, Hamdard J, Döner B, Çıkrıkçıoğlu MA, et al. Protective effect of dexpanthenol against nephrotoxic effect of amikacin: an experimental study. Biomed Pharmacother 2017; 89: 1409-14.

19. Altindag O, Erel O, Soran N, Celik H, Selek S. Total oxidative/anti-oxidative status and relation to bone mineral density in osteoporosis. Rheumatol Int 2008; 28: 317-21.

20. Erel O. A novel automated direct measurement method for total antioxidant capacity using a new generation, more stable ABTS radical cation. Clin Biochem 2004; 37: 277-85.

21. Erel O. A new automated colorimetric method for measuring total oxidant status. Clin Biochem 2005; 38: 1103-11.

22. Xu Y, Ma H, Shao J, Wu J, Zhou L, Zhang Z, et al. A role for tubular necroptosis in cisplatin-induced AKI. J Am Soc Nephrol 2015; 26: 2647-58.

23. Gómez H, Kellum JA. Sepsis-induced acute kidney injury. Curr Opin Crit Care 2016; 22: 546-53.

24. Poston JT, Koyner JL. Sepsis associated acute kidney injury. BMJ 2019; 364: k4891.

25. Mukherjee S, Karmakar S, Babu SP. TLR2 and TLR4 mediated host immune responses in major infectious diseases: a review. Braz J Infect Dis 2016; 20: 193-204.

26. Jochmans I, Nicholson ML, Hosgood SA. Kidney perfusion: some like it hot others prefer to keep it cool. Curr Opin Organ Transplant 2017; 22: 260-6.

27. Bilgic Y, Akbulut S, Aksungur Z, Erdemli ME, Ozhan O, Parlakpinar H, et al. Protective effect of dexpanthenol against cisplatin-induced hepatotoxicity. Exp Ther Med 2018; 16: 4049-57.

28. Zheng C, Wu D, Shi S, Wang L. miR-34b-5p promotes renal cell inflammation and apoptosis by inhibiting aquaporin-2 in sepsis-induced acute kidney injury. Ren Fail 2021; 43: 291-301.

29. Lin Q, Geng Y, Lin S, Tian Z. Sirtuin1 (SIRT1) regulates tumor necrosis factor-alpha (TNF-α-Induced) aquaporin-2 (AQP2) expression in renal medullary collecting duct cells through inhibiting the NF-κB pathway. Med Sci Monit Basic Res 2016; 22: 165-74.

30. Fodor A, Tiperciuc B, Login C, Orasan OH, Lazar AL, Buchman C, et al. Endothelial dysfunction, inflammation, and oxidative stress in COVID-19-mechanisms and therapeutic targets. Oxid Med Cell Longev 2021; 2021: 8671713.

31. Yang B, Lan S, Dieudé M, Sabo-Vatasescu JP, Karakeussian-Rimbaud A, Turgeon J, et al. Caspase-3 is a pivotal regulator of microvascular rarefaction and renal fibrosis after ischemia-reperfusion injury. J Am Soc Nephrol 2018; 29: 1900-16.